ChemComm
Chemical Communications

Accepted Manuscript

This article can be cited before page numbers have been issued, to do this please use: S. Pahar and G. Maayan, *Chem. Commun.*, 2026, DOI: 10.1039/D6CC01564F.

ROYAL SOCIETY OF CHEMISTRY

rsc.li/chemcomm

ChemComm

View Article Online
DOI: 10.1039/D6CC01564F

COMMUNICATION

A Co-peptoid electrocatalyst for nitrite reduction that enables selective production of ammonia

Suraj Pahar [a] and Galia Maayan*[a]

Received 00th January 20xx,
Accepted 00th January 20xx

DOI: 10.1039/x0xx00000x

An intramolecular bio-inspired Co(III) peptoid complex performs as a stable and efficient molecular catalyst for selective electrocatalytic nitrite reduction to ammonia in neutral phosphate buffer, with Faradaic efficiency of 90%. The high selectivity is enabled due to hydrogen bonding by an ethanolic side chain, coupled with phosphate buffer-mediated proton transfer.

The two-steps reduction of nitrite (NO_2^-), a harmful byproduct of ammonia-based fertilizer,[1,2,3,4] to ammonia ($NO_2^- + 5H^+ + 4e^- \rightarrow NH_2OH + H_2O$; $NH_2OH + 3H^+ + 2e^- \rightarrow NH_4^+ + H_2O$) is efficiently catalyzed by cytochrome C nitrite reductase (CcNiR), a multi-haem enzyme, found in various microorganisms, including Desulfovibrio desulfuricans, Wolinella succinogenes and S. deleyianum.[5a] This enzyme contains an iron porphyrinoid active site[5b] embedded within an enzymatic second coordination site comprising histidine, arginine and tyrosine residues, These amino acids play a crucial role in facilitating multielectron and multiproton-transfer steps, as well as acting as a hydrogen bonding network.[6] Inspired by CcNiR, several molecular nitrite-reducing electrocatalysts containing non-precious earth-abundant first-row transition metals (mainly Fe[7-8], Co[9-10], Ni[11] and Cu[12]) have been reported, however, most of these catalysts rely predominantly on first coordination sphere effects as, offering limited control over substrate binding, proton delivery, and intermediate stabilization, which result in strong competition of side reactions such as hydrogen evolution, thus leading to low selectivity to ammonia. Taking this together with the multiple proton- and electron-transfer steps, which enable the formation of multiple possible products such as NO, N_2O, NH_3/NH_4^+, and NH_2OH,[13] selective nitrite reduction to ammonia remains a challenge.

Herein we capitalized on our vast expertise in using synthetic peptide mimics called peptoids[14-15]– N-substituted glycine oligomers – to create and explore second coordination sphere effects within cobalt-based nitrate reduction electrocatalysts. Peptoids are constructed from primary amines and can be easily synthesized on a solid support via the "sub-monomer" method,[16] which enables the site-specific incorporation of diverse side chains, including metal-binding ligands, structure directing elements and photon shuttlers that mimic second coordination sphere effects and can acts as H-bonding donor without altering the primary coordination sphere of the metal ion.[17] Moreover, peptoids are chemically inert to many catalytic transformations, are highly stable over a wide pH range,[18] and can effectively stabilize metal ions in their high and low oxidation states[19] and thus represent a versatile platform for the development of bio-inspired catalysts.[20] We previously demonstrated that non-catalytic side chains incorporated within catalytic metallopeptoids can mimic second coordination sphere effects, improving the efficiency of the catalysts in various oxidative transformations,[21-22] including electrocatalytic water oxidation (WO),[23-26] and increasing the overall stability of the catalytic system. Among these is the peptoid trimer (**TBE**, Fig. 1**)** containing 2,2';6',2"-terpyridine (Terpy) and 2,2′-bipyridine (Bipy), for intramolecular cobalt (Co) coordination, and an ethanolic side chain, that together with the peptoid backbone aimed to serve as a second coordination sphere mimic about the Co centre. The Co complex of this prptoid, Co**TBE** (Fig. 2), demonstrated notable catalytic activity and stability for electrocatalytic and photocatalytic WO in phosphate buffer solution (PBS) at pH 7.[27-28] Inspired by these results, we wished to utilize Co**TBE** as an efficient functional mimic of CcNiR and to explore its electrocatalytic nitrite reduction activity. We anticipated that the –OH group from the ethanolic side will stabilize the catalytic system through hydrogen-bonding interactions, while the phosphate buffer, having multiple protonation states ($H_2PO_4^-$ / HPO_4^{2-}) and low pK_a values, will enable effective proton-coupled electron transfer (PCET) through H-bonding networks and act as an outer-sphere proton shuttler during the electrocatalytic reduction.

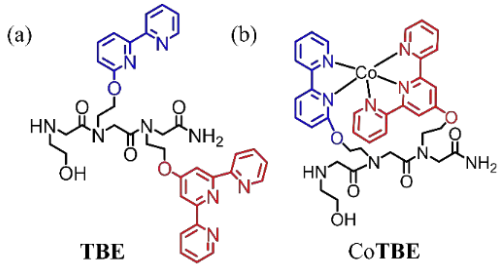

Fig 1. (a) Peptoid ligand **TBE** and (b) the cobalt-peptoid complex Co**TBE**.

[a] Schulich Faculty of Chemistry, Technion–Israel Institute of Technology, Haifa, 3200008, Israel.

TBE and Co**TBE** were synthesized and characterized following our previously reported procedure,[27] and Co**TBE** was subjected to cyclic voltammetry (CV) in PBS pH 7 using a glassy carbon (GC) as the working electrode together with Ag/AgCl reference electrode and a Pt wire as the counter electrode. During the anodic sweep, Co**TBE** displayed two redox events at $E_{1/2}$ values of ~ 0.26 V and ~ -0.77 V vs SHE in PBS pH 7, assigned as the $Co^{III/II}$ and $Co^{II/I}$ couples respectively (Fig. 2). Following these measurements, excess $NaNO_2$ was added to the same solution mixture. The CV performed in presence of excess $NaNO_2$ showed a sharp cathodic wave with an onset potential of about -0.71 V and a peak at -1.03 V vs SHE (Fig. 2), associated with the catalytic event overlapping the reduction of $Co^{II/I}$ redox couple (Fig.S1). Importantly, under identical condition in the absence of NO_2^- or when NO_2^- was replaced by NO_3^-, no such catalytic peak current was observed, demonstrating that the current is associated with the catalytic reduction of NO_2^- but not with the reduction of H^+ to H_2 or of NO_3^- , indicating that Co**TBE** acts as a selective electrocatalyst to NO_2^- reduction. Moreover, CVs recorded in variable concentrations of NO_2^- showed that the catalytic peak current increases with increasing nitrite concentration, indicating that the catalysis is initiated by reduction of nitrite-coordinated Co**TBE** complex (Fig. S2).[28] To confirm the coordination of nitrite with Co**TBE**, we have performed UV-vis experiment in presence of nitrite. Upon addition of the CoTBE to $NaNO_2$, the UV–Vis absorption band at 355 nm for nitrite undergoes a slight blue shift to 352 nm, indicative of changes in the coordination environment upon the formation of nitrite-Co**TBE** complex (Fig. 3a). This is further supported by ESI–MS, which exhibits a mass peak at m/z = 810.75 corresponding to the mass of the nitrite-Co**TBE** complex (Fig. S3). Additionally, UV-vis spectra of solutions containing different Co**TBE** concentrations in the presence of nitrite were recorded. These spectra revealed that the absorption bands linearly vary with the complex concentration following the Beer–Lambert law, which indicates that the complex exists as a single species in this condition (Fig. S4 & S5).[29]

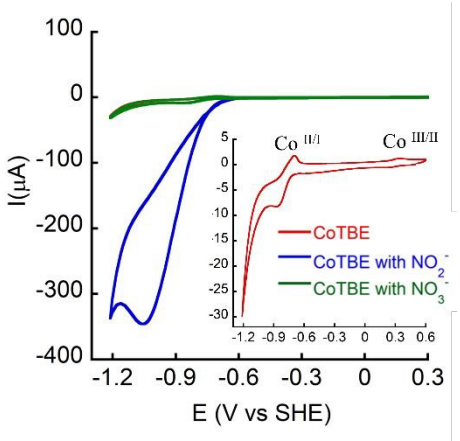

Fig 2. CV of 0.5 mM Co**TBE** (inset, red line) in the presence of 100 mM nitrite (blue) or nitrate (green). All the CVs were performed in 0.1 M phosphate buffer at pH 7, using Ag/AgCl as the reference electrode, glassy carbon as the working electrode (0.07 cm2) and a Pt wire as the counter electrode.

To calculate the TON and faradic efficiency (FE) of the reaction, controlled potential electrolysis (CPE) experiment was performed with 0.5 mM Co**TBE** in 0.1M PBS at pH 7 containing 100 mM $NaNO_2$ using porous glassy carbon as the working electrode. The CPE experiment was carried out at an applied potential of -0.85 V vs SHE (corresponding to $E_{cat/2}$, Fig. S6) for 2 hours in presence and the absence of Co**TBE** (Fig. 3b). During that time, about 37.6 C were accumulated in the presence of Co**TBE** and 10.3 C in the absence of Co**TBE**. Following the CPE, the reaction solution was analyzed using standard colorimetric method to quantify the amount of the generated products specifically NH_4^+ and NH_2OH (Fig. S7 and S8).[30] From this analysis we calculated that $3.66x10^{-5}$ moles of NH_4^+ were produced during the CPE experiment (82% of the total products) while only $8.18x10^{-6}$ moles of NH_2OH (18%) were produced in the same experiment (Fig. S9), indicating that the reduction process catalyzed by Co**TBE** is highly selective to the production of ammonia. Taking the charge accumulation and the moles of NH_4^+ and NH_2OH produced in the presence and absence of Co**TBE** we could calculate a FE of about 78% and 12% respectively, corresponding to the overall FE of about 90% and a total TON of 18 In 2 hrs (Table S1). These results are comparable with the reported literature (Table S2).

Furthermore, CPE studies reveal that nitrite reduction produces NH_2OH and NH_4^+, suggesting a stepwise reduction mechanism with NH_2OH as an intermediate. However, control experiments performed in the presence of NH_2OH instead of nitrite showed no catalytic reduction (Fig. S10), indicating that free NH_2OH is not involved in further reduction steps. Moreover, ESI-MS did not show any detectable Co–NH_2OH adducts (Fig. S11), suggesting the absence of such coordination in solution. These findings indicate that NH_2OH is likely generated as a transient intermediate during catalysis and undergoes further reduction to NH_4^+ only in situ.

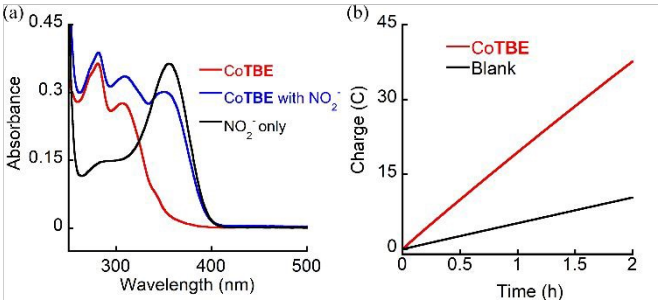

Fig 3. (a) UV–Vis spectra of Co**TBE** complex in the presence and absence of $NaNO_2$ in 0.1 M phosphate buffer at pH 7. (b) Charge passed during CPE at -0.85 V vs SHE for 2 hrs containing 100 mM $NaNO_2$ with Co**TBE** (red) and without (black) in 0.1 M phosphate buffer pH 7, porous carbon as working electrode.

To rule out the possible formation of nanoparticles during the reaction, we carried out dynamic light scattering (DLS) measurement of the reaction solution before and after the CPE and found that they are identical, supporting homogeneous catalysis (Fig. S12). To prove that nitrite reduction does not proceed spontaneously, we stirred a solution of 0.5 mM Co**TBE** and 100 mM $NaNO_2$ in PBS at pH 7.0 for 2 hrs without applying a potential. Post-reaction analysis revealed no

detectable NH_4^+ or NH_2OH formation, indicating that nitrite reduction occurs only under an applied potential (Fig. S13).

To gain some insight about the structural stability of Co**TBE** during nitrite reduction, we performed CV, UV-Vis, FTIR and ESI-MS analysis before and after the CPE experiment. The CV recorded after adjusting the pH of the post-CPE solution showed a decrease in intensity of the catalytic wave along with more negative shift in the onset potential (Fig. S14). These observations indicate the formation of some less active or inactive species during CPE, likely due to structural changes of the complex. In addition, significant change in C–N (~1100 to 1400 cm^{-1}) bond stretching region was observed in post-CPE FTIR spectra (Fig.15), associated with structural changes in Co**TBE** during catalysis. Moreover, notable changes were observed in the UV-Vis spectrum of Co**TBE** after electrolysis, and these further support the structural changes during CPE (Fig.16). Importantly, the absence of particle formation as confirmed by DLS study, together with changes observed in CV, FTIR and UV-vis, indicate that Co**TBE** retains its homogeneous molecular nature. However, the lower catalytic activity after the CPE indicates partial conversion to inactive species formation during catalysis and is consistent with our previous finding in electrocatalytic water oxidation, suggesting dissociation of the Bipy ligand from the Co centre during nitrite reduction.[27] The formation of the inactive species was further confirmed by ESI-MS analysis. The post CPE solution showed masses of 975.6 and 1017.85 corresponding to the masses of [Co**TBE** + $2NO_2^-$ + $H_2PO_4^-$ + Na^+ - H^+] and [Co**TBE** + $2NO_2^-$ + H_2O + $H_2PO_4^-$ + $2Na^+$], respectively. These results provide an additional evidence for the dissociation of Bipy from the Co centre, suggesting that the dissociated Bipy ligand is replaced by H_2O, H_2PO_4, NO_2^- or their combination (Fig.17-18).

Furthermore, the stability of Co**TBE** in the presence of nitrite in PBS at pH 7 was monitored by UV-vis spectroscopy for 24 hours, revealing a notable change in UV-vis spectra over time (Fig. S19), indicating structural changes of the complex in these conditions. Our previous study revealed that this complex is highly stable in PBS pH 7, and therefore we suggest that these changes are associated with nitrite-induced structural modification.[27a] To verify the dissociation of the bipyridine site, we followed the addition of Co, Zn or Ni to Co**TBE** that was stirred for 24 h with nitrite and by UV-vis titration. We observed that only upon addition of Ni, two distinct new absorption bands appeared near ~314 nm and ~328 nm (Fig. 4a and S20), corresponding to the metal coordination to Bipy, indicating that this has become an open binding site probably due to nitrite-induced ligand dissociation and the replacement of Bipy by nitrite species. [27a] Moreover, HR-MS of the isolated solution of UV-vis titration experiments with Ni showed a peak at m/z = 863.26 corresponding to the mass of [CoNi**TBE** + H_2O + Na^+] (Fig. 21) indicating the selective Ni coordination to the dissociated Bipy ligand. The FTIR-spectrum of dried complex after 24 h in the presence of nitrite, exhibited additional bands in the 1500 - 1030 cm^{-1} region, along with notable shifts in the C–N and C=N stretching regions (Fig. S22), providing further evidence for the dissociation of Bipy in the presence of NO_2^-.

To assure that Co**TBE** acts as a soluble molecular catalyst and to rule out any possible involvement of insoluble nanoparticles or surface adsorbed species formation during the electrocatalytic nitrite reduction, a rinse test was performed, in which 20 continuous CV scans were carried out in PBS (pH 7) containing 0.5 mM Co**TBE** and 100 mM $NaNO_2$ using GC as working electrode (Fig. S23). Thereafter, the GC electrode was rinsed gently with deionized water and dried. A subsequent CV scan was performed in a fresh PBS containing only 100 mM $NaNO_2$ using this electrode. The resulting CV showed no catalytic current and was almost identical to the CV scan in PBS (pH 7) containing only 100 mM $NaNO_2$, indicating the absence of deposited insoluble catalytic species on the electrode surface.[31]

To identify the possible role of phosphate buffer as a proton donor for electrocatalytic nitrite reduction, we have performed CV experiments under identical condition in 3-morpholinopropane-1-sulfonic acid (MOPS) and 4-morpholineethanesulfonic acid (MES) buffers. These two buffers were previously successfully used as solution media in electrocatalytic nitrite reduction.[9b] CV experiments revealed that the catalytic peak current is much lower and the onset potential for the catalytic event is much higher in both MOPS and MES buffers compared to those measured in PBS (Fig. S24), indicating a lower catalytic activity. Furthermore, to confirm the role of phosphate buffer a series of CV scans in different buffer concentrations (0 - 100 mM) was conducted (Fig. S25). The peak current of the catalytic wave was found to clearly increase with increasing the buffer concentration at constant nitrite concentration, indicating the active participation of the buffer ions in the catalytic nitrite reduction, likely by facilitating the proton transfer steps through effective proton shutteling.[32] Subsequently, to prove the involvement of proton-mediate pathways in catalytic nitrite reduction, CV experiments were performed under identical conditions in buffered solution using H_2O and D_2O as solvent (Fig. S26). A substantially lower catalytic peak current was observed in D_2O, highlighting the crucial role of proton transfer steps to facilitate nitrite reduction. Taking together the observations from all these experiments, we can suggest that the role of the phosphate buffer ions is to actively participate in the proton transfer and facilitate it.

To explore the role of the ethanolic side chain we used two previously synthesized control Co-peptoid complexes; one containing a benzyl group side chain instead of the ethanolic side chain (Co**TB-BZ**), and the second having no additional side chain at the N-terminal (Co**TB**). Although the catalytic activity of both complexes was similar to that of Co**TBE** under identical condition (Fig. 4b), a rinse test experiment using the two control complexes revealed their instability during the electrocatalytic reaction; after 20 continues CV scans followed by subsequent electrode rinsing, these two complexes persist activity, indicating deposition of catalytically active species on the electrode surface (Fig. S27 and S28). These results demonstrate that although the ethanolic side chain not directly assist in enhancing the catalytic activity, it does play a key role in stabilizing the overall system during electrocatalytic nitrite reduction, assumingly through H-bonding interaction.

A kinetic study revealed that the catalytic peak current (i_{cat}) of nitrite reduction varies linearly with increasing Co**TBE** concentration in the presence of NO_2^- (Fig. S29) .[32] This first order kinetics suggests a single site mechanism for nitrite reduction.[33] Additionally, i_{cat} showed a linear relationship with square root of the scan rates, confirming that the Co**TBE**-catalyzed nitrite reduction process follows diffusion-controlled kinetics (Fig. S30).[34]

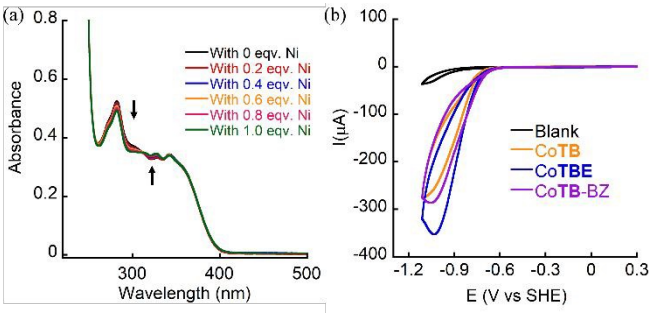

Fig 4. (a) UV-Vis titration spectra of the solution containing 20 μM of Co**TBE** with $NaNO_2$ in 0.1M phosphate buffer at pH 7 after 24 hours of undisturbed incubation with Ni, (b) CV of 0.5 mM Co**TBE**, Co**TB-BZ,** Co**TB** and without catalyst, all the CV scans were performed in 0.1 M phosphate buffer at pH 7 containing 100 mM nitrite.

In recent decades, the increase in environmental nitrite levels caused by uncontrolled industrial waste and a significant overuse on nitrogen-based fertilizers in agriculture is causing significant imbalance in the global N-cycle, creating major human health issues. Inspired by CcNiR, we describe here the first metallo-peptidomimetic complex that is a functional mimic of CcNiR and demonstrate its ability to facilitate electrocatalytic nitrite reduction towards selective formation of ammonia with an overall FE of ~ 90%. Moreover, we show that the ethanolic side chain, located near the catalytic Co centre, functions as a H-bonding donor thus acting as second coordination sphere mimic, while the phosphate buffer serves as proton shuttler that facilitates the proton transfer step during electrocatalytic nitrite reduction (Fig. 5). Overall, our study represents a step forward in the development of stable and efficient biomimetic catalysts that can facilitate multiproton, multielectron nitrite reduction reaction to ammonia with high selectivity.

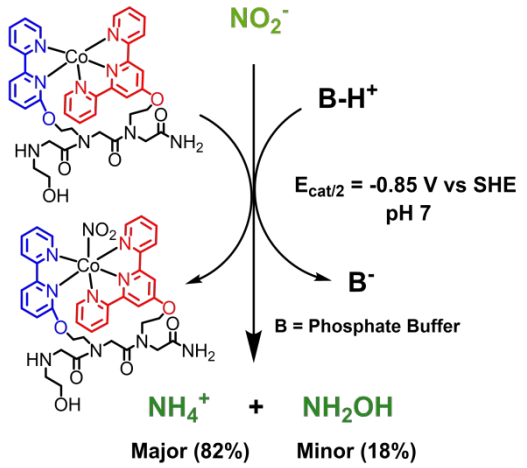

Fig 5. Proposed scheme for electrocatalytic nitrite reduction by Co**TBE** in PBS at pH 7.

Conflicts of interest

View Article Online
DOI: 10.1039/D6CC01564F

There are no conflicts to declare.

Data availability

All data supporting the findings or analysed of this study are available in the article and its supplementary information (SI).

Acknowledgements

The authors thank Mrs. Nicole Vorobyov for fruitful discussions and Mrs. Orr Bar-Natan for assistance with the DLS experiments.

References

1. C. J. Stevens, *Science.* 2019; **363** (6427), 578-580.
2. J. W. Erisman, M. A. Sutton, J. Galloway, Z. Klimont, W. Winiwarter, *Nat. Geosci.* 2008, **1**, 636.
3. S. Matassa; D. J. Batston; T. Hülsen; J. Schnoor; W. Verstraete, *Environ. Sci. Technol.* 2015, **49**, 5247− 5254.
4. J. G. Morrissy, M. J. Currell, S. M. Reichman, A. Surapaneni, M. Megharaj, N. D. Crosbie, D. Hirth, S. Aquilina, W. Rajendram, A. S. Ball, *Earth-Sci.Rev.* 2021, **222**, 103816.
5. (a) O. Einsle, A. Messerschmidt, P. Stach, G. P. Bourenkov, H. D. Bartunik, R. Huber, P. M. H. Kroneck, Nature 400, 476–480 (1999), (b) E. T. Judd, N. Stein, A. A. Pacheco and S. J. Elliott, *Biochemistry*, 2014, **53**, 5638 — 5646.
6. O Einsle, A Messerschmidt, R Huber, P. M. H. Kroneck, F Neese, *J. Am. Chem. Soc*., 2002, **124**, 11737-11745.
7. Y. W. Chi, J. Y Chen, K. Aoki, *Inorg. Chem*. 2004, **43**, 8437−8446.
8. M. H. Barley, K. J. Takeuchi and T. J. Meyer, *J. Am. Chem. Soc.,* 1986, **108**, 5876 —5885.
9. (a) S. Xu, D. C. Ashley, H. Y. Kwon, G. R. Ware, C. H. Chen, Y. Losovyj, X. Gao, E. Jakubikova and J. M. Smith, *Chem. Sci*., 2018, **9**, 4950 —4958, (b) S. Partovi, E. Z. Dalton and J. M. Smith, ACS Catal. 2024, 14, 10, 7756−7761.
10. I. Taniguchi, N. Nakashima, K. Yasukouchi, *J. Chem. Soc., Chem. Commun.* 1986, 1814−1815.
11. (a) J. Ferguson, J. Brown and D. Richeson, ChemCatChem, 2024, e202301168, 1 —8, (b) S. Norouzinyanlakvan, J. Ovens and D. Richeson, Catal. Sci. Technol., 2024, 14, 5422–5429.
12. (a) J. G. Woollard-Shore, J. P. Holland, M. W. Jones, J.R. Dilworth, Dalton Trans. 2010, **39**, 1576−1585, (b) G. Cioncoloni, I. Roger, P. S. Wheatley, C. Wilson, R. E. Morris, S. Sproules and M. D. Symes, ACS Catal., 2018, **8**, 5070 — 5084.
13. S. Amanullah, P. Saha, A. Nayek, M. E. Ahmed and A. Dey, *Chem. Soc. Rev.*, 2021, **50**, 3755 —3823.
14. J. Seo, B.-C. Lee and R. N. Zuckermann, Comprehensive Biomaterials, P. Ducheyne, K. E. Healy, D. W. Hutmacher, D. W. Grainger and C. J. Kirkpatrick, Elsevier, Amsterdam, 2011, vol. vol. 2, pp. 53–76,

View Article Online
DOI: 10.1039/D6CC01564F

15. G. Maayan Eur. J. Org Chem., 2009, 5699 —5710.
16. R. N. Zuckermann , J. M. Kerr , S. B. H. Kent and W. H. Moos , *J. Am. Chem. Soc.*, 1992, **114**, 10646.
17. G. Maayan, M. D. Ward and K. Kirshenbaum, *Chem. Commun.,* 2009, **1**, 56 —58, (b) M. Baskin, H. Zhu, Z. W. Qu, J. H. Chill, S. Grimme and G. Maayan, *Chem. Sci.,* 2019, **10**, 620 —632, (c) N. Vorobyov and G. Maayan, Chem. Eur. J. 2025, **31**, e202500693.
18. H. R. Reese, C. C. Shanahan, C. Proulx and S. Menegatti, *Acta Biomater.*, 2020, **102**, 35 —74.
19. (a) A. D'Amato, P. Ghosh, C. Costabile, G. Della Sala, I. Izzo, G. Maayan and F. De Riccardis, *Dalton Trans*., 2020, **49**, 6020–6029, (b) A. E. Behar and G. Maayan, Chem. Eur. J. 2023, **29**, e202301118.
20. (a) R. Schettini, B. Nardone, F. D. Riccardis, G. D. Sala and I. Izzo, *Eur. J. Org Chem.,* 2014, 7793 —7797, (b) D. Chandra Mohan, P. Ghosh, T. Ghosh and G. Maayan, *Chem.–Eur. J.*, 2020, **26**, 9573 —9579.
21. K. J. Prathap and G. Maayan, *Chem. Commun.,* 2015, **51**, 11096,
22. D. C. Mohan, A. Sadhukha and G. Maayan, *J. Catal.,* 2017, 3355,139
23. T. Ghosh, P. Ghosh and G. Maayan, *ACS Catal*., 2018, **8**, 10631
24. (a) G. Ruan, P. Ghosh, N. Fridman and G. Maayan, *J. Am. Chem. Soc.*, 2021, **1143**,10614 —10623, (b) G. Ruan, S. Pahar, N. Fridman and G. Maayan, Inorg. Chem. 2025, 64, 9, 4267–4274.
25. G. Ruan, L. Engelberg, P. Ghosh and G. Maayan, *Chem. Commun*., 2021, **57** ,57, —942,
26. S. Pahar, K. Majee and G. Maayan *Eur. J. Inorg.Chem.* 2024, **27**, e2023005.
27. (a) S. Pahar and G. Maayan, *Chem. Sci*., 2024, **15**, 12928-12938, (b) S. Pahar, K. Majee and G. Maayan, *ACS Omega*, ACS Omega 2026, 11, 8, 12992–12999.
28. Y. Guo , J. R. Stroka , B. Kandemir , C. E. Dickerson and K. L. Bren , *J. Am. Chem. Soc*., 2018, **140**, 16888 —16892.
29. J. Shen, X. Zhang, M. Cheng, J. Jiang and M. Wang, *ChemCatChem,* 2020, **12**, 1302 —1306.
30. (a) M. W. Weatherburn, *Anal. Chem*. 1967, **39**, 971– 974. (b) D.S. Frear, and R.C.Burrell , *Anal. Chem*. 1955, 27(**10**), 1664-1665.
31. (a) D. J. Wasylenko, R. D. Palmer, E. Schott and C. P. Berlinguette, Chem. Commun., 2012, 48, 2107 —2109, (b) P. K. Das, S. Bhunia, P. Chakraborty, S. Chatterjee, A. Rana, K. Peramaiah, M. M. Alsabban, I. Dutta, A. Dey and K.-W. Huang, Inorg. Chem., 2021, 60, 614 —622.
32. S.E. Braley, H.Y. Kwon, S. Xu, E.Z. Dalton, E. Jakubikova, and J.M. Smith, *Inorg. Chem.* 2022, **61**,12998-13006.
33. F. S. Yu, F. Li, J. X. Hu, L. C. Bai, Y. Zhu and L. C. Sun, *Chem. Commun*., 2016, **52**, 10377.
34. N. Elgrishi, K. J. Rountree, B. D. McCarthy, E. S. Rountree, T. T. Eisenhart and J. L. Dempsey, *J. Chem. Educ.*, 2018, **95**, 197 —206.

View Article Online
DOI: 10.1039/D6CC01564F

Data availability

All data supporting the findings or analysed of this study are available in the article and its supplementary information (SI).